Surface modification of MWCNT and its influence on properties of paraffin/MWCNT nanocomposites as phase change material

Arezoo Avid[1], Seyed Hassan Jafari[1*], Hossein Ali Khonakdar[2,3], Mehdi Ghaffari[4], Beate Krause[3], Petra Pötschke[3]

[1]School of Chemical Engineering, College of Engineering, University of Tehran, P.O. Box: 11155-4563, Tehran, Iran

[2]Department of Polymer Processing, Iran Polymer and Petrochemical Institute, P.O. Box: 14965-115, Tehran, Iran

[3]Leibniz Institute of Polymer Research Dresden, Hohe Straße 6, Dresden D-01069, Germany

[4]Polymer Engineering Department, Golestan University, Postal Code: 49138-15739, Gorgan, Iran

Abstract

Multi-walled carbon nanotubes (MWCNTs) were modified by an organo-silane in order to improve their dispersion state and stability in paraffin wax. A family of paraffin-based phase change material (PCM) composites filled with MWCNTs was prepared with different loadings (0, 0.1, 0.5, 1 wt.%) of pristine MWCNTs and organo-silane modified MWCNTs (Si-MWCNT). Structural analyses were performed by means of Fourier transform infrared (FTIR), scanning electron microscopy (SEM) and rheological studies using temperature sweeps. Moreover, phase change transition temperatures and heat of fusion as well as thermal and electrical conductivities of the developed PCM nanocomposites were determined. The SEM micrographs and FTIR absorption bands appearing at ca. 1038 cm^{-1} and 1112 cm^{-1} confirmed the silane modification. Differential scanning calorimetery (DSC) results indicated that the presence of Si-MWCNTs leads to slightly favorable enhancement in the energy storage capacity at the maximum loading. It was also shown that the thermal conductivity of the PCM nanocomposites, in both solid and liquid phases, increased with increasing the MWCNT content independent of the kind of MWCNTs by up to about 30% at the maximum loading of MWCNTs. In addition, the modification of MWCNTs made the samples completely electrically nonconductive, and the electrical surface resistivity of the PCMs containing pristine MWCNTs decreased with increasing MWCNTs loading. Furthermore, the rheological assessment under consecutive cyclic phase change demonstrated that the samples containing modified MWCNTs are more stable compared to the PCM containing pristine MWCNTs.

Keywords: Phase change material; Multi-walled carbon nanotubes; Paraffin; Organosilane; Thermal energy storage

---

*Corresponding author: S.H. Jafari (shjafari@ut.ac.ir)

1. Introduction

In the 21st century, rapid depletion of fossil fuels, concerns over greenhouse gas production, and growing environmental concerns make the effective utilization of energy a critical issue [1]. The growing economics and population since the industrial revolution, and the mismatch between energy supply and demands create the need of exploiting renewable and sustainable energy sources, such as water, wind, and solar, toward an affordable energy technology in future [2,3]. Since the intermittent nature of clean energy sources, the total energy consumption can be reduced substantially with the implementation of highly efficient thermal storage materials and devices. Thermal energy storage (TES) is one such technology which provides very specific solutions [4].

In many parts of the world, direct solar radiation is considered to be one of the most prospective sources of energy. Solar energy is available only during the day, and hence, its application requires efficient thermal energy storage so that the excess heat collected during sunshine hours may be stored for later use during the night [5,6]. Sensible heat storage (SHS) method is most commonly used for solar energy applications; however, latent heat storage (LHS) offers a much higher storage density with a narrower temperature range between storing and releasing heat [1]. Latent heat thermal energy storage (LHTES) using phase change materials by the means of solid–liquid transitions offers an attractive way for the effective use of thermal energy [7]. Phase change materials (PCMs) store thermal energy through the loosening or breaking apart of molecular or atomic bond structures when energy is transferred into the material, and while they undergo a phase transition, they can keep the surroundings at a constant temperature. The stored heat can be discharged into the environment at a later time as the material recrystallizes [8]. PCMs have been widely incorporated in thermal storage of solar energy, thermal protection of food, temperature maintenance in rooms with computers or electrical appliances, passive storage in bioclimatic buildings, medical applications, cooling of engines etc. [9].

A great number of materials have been examined as candidate PCMs that can be classified into two categories, namely organic and inorganic. As an organic PCM, paraffin wax (PW) has attracted numerous attentions because of its large latent heat and proper thermal characteristics such as little or no super cooling, low vapor pressure in the melt, good thermal and chemical stability, self-nucleating behavior, safety, and commercial availability at low cost [10,11]. However, one of the inherent drawbacks of paraffin is its low thermal conductivity (≅0.2 W/m K) [5], which decelerate the rate of absorbing and releasing heat. To overcome this problem, a wide range of investigations was conducted to improve the thermal conductivity of the paraffin based PCMs.

A common method is to disperse solid nanoparticles with high thermal conductivity to form composite PCMs [12]. Among the various nanofillers examined, carbon nanomaterials such as single and multi-walled carbon nanotubes (SWCNTs, MWCNTs), carbon blacks, and exfoliated graphite nanoplatelets, with intrinsically high conductivities and relatively low densities, have been preferred in making nano-enhanced PCMs because they become electrically and thermally conductive at low loadings of these nanoparticles [13,14].

Carbon nanotubes (CNTs) possess many desirable properties suitable for the PCM application due to their high thermal conductivity, electrical capacity, thermal stability, and large aspect ratio [15]. Molecular dynamics (MD) simulations suggest an unusually high value of thermal conductivity (λ =6600 W/mK) for an isolated CNT at room temperature, comparable to a hypothetical isolated graphene monolayer or graphite [16]. The aspect ratio of the filler dictates the conductivity of a composite as random bridges or networks are formed from conductive particles at lower loading when filler with higher aspect ratio is used. Higher aspect ratio results in reduced contact resistance and facilitates electron and phonon transfer. Therefore, with their aspect ratio ranging from 100 to 1000, MWCNTs are one of the best candidates for this purpose [17].

On the other hand, CNTs are usually entangled and not readily dispersed into organic matrices. Hence, many different surface treatments and functionalization techniques have been devised for improving the dispersion and interfacial adhesion of CNTs with various polymer matrices [18]. Silanization is a preferred method which provides an approach to add different organic molecules to CNT surfaces not only to diversify their surface behavior, but also to incorporate a variety of chemical moieties depending on the coupled organosilanes. It thus opens the opportunity to use the silane function as a coupling agent of different organic compounds and polymer matrices [19].

Fang et al. [2] studied TES performance of paraffin-based composite PCMs filled with hexagonal boron nitride (h-BN) nanosheets in the absence of any surfactants and found that the thermal conductivity of the PCM increased by a factor up to 60% with raising the loading of h-BN nanosheets up to 10wt%. However, the composite PCMs became unstable with significant precipitation of h-BN nanosheets upon consecutive cyclic solid–liquid phase change. In one study, Wang et al. [20] embedded pristine MWCNTs into the paraffin and showed that in the composite containing 2.0wt%, the thermal conductivity enhancement ratios reached 35% and 40% in solid and liquid states, respectively. Teng et al. [21] added MWCNTs and graphite to paraffin to enhance the thermal properties of PCMs. Their experimental results demonstrated that adding the MWCNTs was more effective than graphite in modifying the thermal storage performance of paraffin for most of the experimental parameters. In another study, Wang et al. [12] treated CNTs by a mechano-chemical reaction. Treated CNTs were successfully dispersed in the palmitic acid matrix due to their hydroxide radical functional groups on the surface of CNTs.

Hashempour et. al [22] employed MWCNTs to improve the thermal properties of butyl stearate as a PCM, and used a surfactant to stabilize the nanotubes in the matrix. The highest reported improvement in thermal conductivity by implementing the surfactant was from 0.16 to 0.185 w/mK at 50ºC.

Wang et al. [23] prepared two different kinds of grafted MWCNTs, and compared the effect of two modifications on thermal properties of the paraffin wax and palmitic acid. By adding low amounts of grafted MWCNTs, they indicated that modification has the potential of improving the thermal conductivity of the PCM at temperatures higher than 60ºC compared to pristine MWCNTs. However, at lower temperatures the modified MWCNT containing nanocomposites showed lower thermal conductivity compared to pristine MWCNTs. In all of the previous works, the study of modification on the stability of paraffin-based nanocomposites which is a major performance limiting factor is missing. Therefore, in this work we focus on providing a novel technical approach for preparing a stable paraffin-based PCM by surface modification of nanofillers, while keeping or enhancing the thermal performance. MWCNTs as nanofillers and octadecyltrimethoxy silane (ODMS) as an organo-silane modifying coupling agent were chosen in order to make high performing and stable nanocomposite PCMs under repeated cyclic phase changes. Thermal energy storage performance of the PCMs including melting/solidification rates, onset temperatures, peak temperatures, and heat of fusion as well as their thermal and electrical conductivities, morphological and rheological characteristics are explored.

2. Experimental

2.1. Materials

Pristine and oxidized MWCNTs (NC3100 and NC3101 grades, respectively) were obtained from Nanocyl SA (Sambreville, Belgium). The average diameters of MWCNTs were 9.5nm and their average lengths were 1.5μm. As PCM matrix, paraffin wax (RT44-HC) was purchased from Rubitherm, with a latent heat of 250 kJ/kg and a nominal melting point of 43ºC. ODMS (90% technical grade) was supplied by Sigma-Aldrich. Acetone and ethanol were obtained from Merck Inc. and used as delivered.

2.2. Sample preparation

2.2.1. Silanization of MWCNTs

For silane treatment of the MWCNTs, 1g of oxidized MWCNTs was first bath-sonicated in ethanol in a three-neck round-bottom flask for 1 h. Thereby, $5*10^{-5}$ $mol.L^{-1}$ of NaOH was added to the suspension as a catalyst prior to reflux. In addition, 5% of water was added to the solution to increase the hydrolysis. 3mL of ODMS was diluted in 10mL of ethanol, and the ODMS/ethanol solution was added to the oxidized MWCNT suspension slowly in 0.5mL increments after the suspension started to reflux. The reaction was under reflux for 5h. The silane-treated MWCNTs (Si-MWCNT) were then vacuum dried, washed with ethanol and acetone to eliminate any un-reacted coupling agent, separated by centrifuge, and finally dried in an oven at 80ºC for 12h. A schematic representation of the silanization process is given in Fig. 1.

Figure 1. Schematic representation of silanization process of multi-walled carbon nanotubes

2.2.2. Preparation of PCM nanocomposites

For preparing PCM composites, paraffin wax was first melted at 45°C. The modified and pristine MWCNTs, at various given loadings, were added into the molten paraffin to form mixtures that were rigorously stirred at 50°C by a magnetic stirrer/hot plate for 1h. Then the mixtures were subjected to intensive ultrasonication which was set at 37Hz and left to run for 1h to prepare well-dispersed MWCNTs within the PCM. The nano-filled PCM was then poured into a cast and allowed to solidify. Nanocomposite PCMs were prepared with 0.1, 0.5 and 1 wt.% of modified and pristine MWCNTs, along with a reference sample (0 wt.%) of neat paraffin.

2.3. Characterization

2.3.1. Fourier transform infrared spectroscopy

Fourier transform infrared (FT-IR) spectra of the oxidized MWCNTs and Si-MWCNTs were recorded using a PerkinElmer-Spectrum Two FTIR spectrometer with KBr pellets, in the frequency range of 400-4000 cm^{-1}.

2.3.2. Scanning electron microscopy (SEM)

To investigate the effect of silane modification on dispersion of MWCNTs morphological characterization of the powder and the composites was performed using SEM by means of a Carl Zeiss Ultra plus microscope. Before imaging, composites were cryo-fractured in liquid nitrogen and the surfaces were coated with 3nm platinum.

2.3.3. Differential scanning calorimetry (DSC)

A DSC Q2000 from TA Instruments was applied, and a high-purity nitrogen atmosphere was used. A sample of around 5 ±1 mg was loaded to the DSC pan. The data were collected for the second heating and cooling runs at a fixed scanning rate of ±10K/min in a temperature range of -80 to 100°C. The solid–liquid transformation, the melting temperature, the crystallization temperature, and enthalpy of fusion (latent heat of fusion) were analyzed. The DSC instrument was calibrated with standard samples of known thermal properties prior to use.

2.3.4. Electrical surface resistivity measurement

The electrical resistivity of paraffin/pristine MWCNTs and paraffin/modified MWCNTs nanocomposites was studied with a Loresta-GP MCP T610 instrument from Mitsubishi Chemical Analytech. As the samples were brittle, they were broken partially, and the specimens were characterized using the four-pin probe method at room temperature. The electrode and probe types were ESP/61403A and ESP, respectively, which are mostly used for non-uniform samples. The measurements were repeated five times for each sample at different locations to obtain the average value with standard deviation. The Resistivity Correction Factor (RCF) was 4.532 and the supplied voltage was 10V.

2.3.5. Thermal conductivity measurement

The KD2 Pro thermal properties analyzer (Decagon Devices, USA) was employed to measure the thermal conductivity K. This instrument is based on the principle of the transient hotwire method. The TR-1 probe sensor was used for the measurements of the solid nanocomposites while it inserted in the designated hole in the samples. Control of measurement temperature was implemented by placing the solid samples in a custom aluminum holder that was submerged in a constant desired temperature bath. The measurements were performed for the samples at temperatures 26ºC and 51ºC and repeated 3 times at each temperature for each one and their average value was used. The detailed measurement principal and procedure have been described elsewhere[13]. The accuracy of the method was about ± 0.05 W/mK.

2.3.6. Temperature sweep rheological analysis

The rheological experiments were performed using temperature sweep by an Anton Paar Physica MCR 300 (Graz, Austria) with parallel-plate geometry (plate diameter 25mm) under nitrogen atmosphere. The temperature was increased from 40ºC to 80ºC in steps of 2K per min. To set a suitable strain for the tests and to ensure that the applied strain did not exceed the limit of linear viscoelasticity, strain sweeps (from 0.01 to 100%) were initially performed for each sample at a fixed frequency of 20rad/s. The temperature sweeps were performed at the strain amplitude of 0.5% to ensure a linear viscoelastic response and a fixed frequency of 20rad/s.

3. Results and Discussion

3.1. FTIR analysis

In order to check the suitability of the MWCNT modification, FTIR was applied at different processing steps. For the oxidized MWCNTs (Fig. 2a), the peaks at 1715 cm^{-1} and 1160 cm^{-1} are assigned to C=O and C-O stretching vibrations of the carboxylic groups (–COOH), respectively. A broad transmission band centered at 3435 cm^{-1} is observed for the OH functionality on the surface of the MWCNTs [24]. The adsorption band at around 1634 cm^{-1} can be attributed to the stretching mode of conjugated C=C- in an enol form [12]. The peak at 501cm^{-1} is due to the presence of impurities and iron catalysts [25].

In Fig.2b, the peaks at 2920 cm^{-1} and 2850 cm^{-1} confirm the presence of C-H sp^3 bonding, indicating hydrocarbon chains on the surface of MWCNTs [26]. The IR spectrum also shows a new peak at 682 cm^{-1} which is attributed to the C-H bending in hydrocarbon chains. The bands at 1038 cm^{-1} and 1112 cm^{-1} are due to Si-O-Si and Si-O-C_{MWCNT} vibrations and correspond to siloxane units formed during the silanization process. The absence of peaks between 815 cm^{-1} and 845 cm^{-1} for treated MWCNTs indicates that all methyl groups of the Si-O-CH_3 in ODMS are not available anymore via the silanization reaction [19].

FTIR results confirm the presence of the silane coating, and there is strong evidence for a change in the chemical structure of the surface of the MWCNTs.

Figure 2. FTIR spectra of a) oxidized and b) silanized MWCNTs

3.2. Morphology and dispersion of MWCNTs

In order to investigate the effect of silanization on the morphology of the composites and the dispersion of MWCNTs, scanning electron microscopy on cryo-fractured surfaces was performed. It is expected to have more homogenous surface when we have better dispersion of nanoparticles [27]. Fig. 3 shows the SEM images of the PCM composites containing 0.5 wt.% of pristine and silanized MWCNTs as a typical example. It is observed that the broken composite surface appears to be more homogenous when Si-MWCNTs were used. Both nanotubes are nicely embedded and cannot be seen on the surfaces. It is expected that the silane coupling agent can improve the adhesion between Si-MWCNTs and the paraffin matrix since the long hydrocarbon chains of ODMS are covalently bonded on the surface of the MWCNTs and has the potential to enhance their compatibility with paraffin. In fact, the incorporation of surface-functionalized MWCNTs results in better dispersion of Si-MWCNTs in the matrix which is the reason of the observed finer morphology.

Figure 3. SEM images of paraffin wax composites loaded with 0.5 wt.% of a) pristine MWCNT b) Si-MWCNT

3.3. Differential scanning calorimetry (DSC) analysis

The DSC technique was used to investigate the influence of MWCNT addition on thermal properties including the melting/solidification temperatures and its capacity to store thermal energy. Both the heating and cooling behaviours of the paraffin nanocomposites were recorded.

Fig.4 presents the DSC thermograms of PW/pristine MWCNT and PW/Si-MWCNT composites. Two separate phase transition peaks are observed on both the heating and cooling curves. The small peak on each curve that occurs at lower temperature corresponds to the solid–solid phase change and the main peak represents solid-liquid phase change [28]. When the PCM undergoes a solid–solid phase change, its molecular structure is altered and the thermal energy is stored due to a change in the molecular bonding structure of the alkane molecules [8].

(a)

Figure 4. DSC curves (cooling and second heating) of the paraffin-based nanocomposite PCMs filled with a) pristine MWCNTs b) Si-MWCNTs

The melting temperatures and latent heat of fusion values for the neat paraffin, pristine and modified MWCNT composite PCMs are summarized in Tables 1 and 2. The relevant enthalpies were calculated by integration of the peaks above the base line given by the TA software itself. For the neat paraffin, the melting and solidification temperatures were determined to be 43.8 ± 0.1 and 41.7 ± 0.1 °C, respectively. The melting temperature is in good agreement with the specified value (43°C) by the supplier. It was found that the melting/solidification temperatures of the composite PCMs are nearly unvaried and independent of the presence of MWCNTs, with the maximum deviation being less than 0.5K. Hence, the temperatures that characterize the melting and crystallization peaks are not affected significantly by the addition of pristine and modified MWCNTs. The observed changes may be attributed to the filler-induced alignment of paraffin molecules surrounding the carbon nanofillers that alters the local steric hindrance, especially at higher loadings [12,26].

Table 1. Heating and cooling characteristics of PCMs containing pristine MWCNTs (average of three samples)

Sample	Melting Peak (°C)	Melting Enthalpy (J/g)	Cryst. Peak $T_{c,\,max}$ (°C)	Cryst. Enthalpy (J/g)
PW	43.8	238.9	41.7	237.2
0.1 wt. %	43.5	240.1	42.0	240.6
0.5 wt. %	43.9	234.3	41.5	232.3
1 wt. %	43.9	232.3	41.7	232.2

Table 2. Heating and cooling characteristics of PCMs containing Si-MWCNTs (average of three samples)

Sample	Melting Peak (°C)	Melting Enthalpy (J/g)	Cryst. Peak $T_{c,\,max}$ (°C)	Cryst. Enthalpy (J/g)
0.1 wt. %	43.9	236.3	41.9	236.6
0.5 wt. %	43.6	236.0	42.2	236.5
1 wt. %	43.7	239.0	41.8	237.9

Although the primary purpose of MWCNT addition is to enhance the thermal conductivity of the PCMs, MWCNTs decrease the energy storage capacity undesirably because it does not melt and solidify within exactly the same phase change temperature range of the base PCM. Hence, the phase change enthalpies of the nanocomposite PCMs loaded with the pristin MWCNTs are mostly lower than those of the neat paraffin wax. The melting enthalpy decreased about 7J/g with the addition of only 1wt.% of prisitine MWCNT. On the other hand, for the PCM composites containing Si-MWCNT not only the energy storage drop with the addition of MWCNTs is overcome, a slightly favourable enhancement both in the melting and solidification enthalpies of is observed for the nanocomposites with 1wt.% of modified MWCNTs. This indicates that silanization has the potential in improving the performance of PCM nanocomposite provided that higher loadings of the silanized MWCNTs are used.

3.4. Electrical resistivity of PCM nanocomposites

MWCNTs are conductive fillers as they possess conjugated π-electrons which can transfer electrical charges [19]. They could greatly improve the electrical properties of composite PCM materials and induce a sharp transition from electrical insulator to electrical conductor behavior. The improvement of the electrical conductivities depends on the formation of particle -particle networks, named percolation [17]. This simply means that a very high percentage of electrons are permitted to flow through the sample due to the creation of an interconnecting conductive pathway.

To check the effect of the modification of MWCNTs and the dispersion at different contents of MWCNTs on the electrical resistivity of the nanocomposites, the surface resistivity of paraffin/un-modified MWCNT and paraffin/modified MWCNT samples was measured and the results are presented in Fig. 5. It is seen that the surface resistivity decreases with the addition of MWCNTs achieving the electrical resistance value (882.7 Ω/square) with 1 wt.%.

Figure 5. Electrical surface resistivity of pristine MWCNT/paraffin PCM nanocomposites

The neat paraffin and composites containing modified MWCNTs were completely nonconductive and showed resistance values above the measuring range of the used equipment (>10 E+7 Ω). This behavior can be explained by two main reasons. First, the MWCNTs underwent a chemical functionalization reaction and the ODMS molecules are covalently bonded to the MWCNT surface. This treatment leads to the formation of numerous defects on both the MWCNT tip-end and sidewalls which is detrimental for electrical properties of nanocomposites [29]. The distortion of the graphitic structure reduces the electrical conductivity of the tubes since the introduction of functional groups into a conjugated π-electron system is combined with the conversion of sp^2-carbons to sp^3-carbons. The structural changes interrupt the conjugation and induce a distortion of the graphitic layer. In terms of the electron conduction, these sp^3-carbons can be regarded as defects and consequently perturb electron transfer [30]. It is to be noted that the detrimental effect of chemical functionalization on the honeycomb structure of MWCNTs can be proved by RAMAN spectra which are not reported here.

In addition, the formation of organic layer wrapping of non-conducting silane on the MWCNT wall surfaces might increase the electrical contact resistance between neighbored nanotubes. This extra substance can be considered as an electrically insulating layer which increases the distance between individual tubes, making the tunneling of electrons from tube to tube more difficult [31].

3.5. Thermal conductivity of PCM nanocomposites

Since the rate of energy storage and release is one of the key performance indicators of PCMs, the thermal conductivity K of the PCMs at both solid and liquid states was measured. Heat transport in nanocomposites occurs by both electrons and heat carrying wave packages (phonons) of varying frequencies, but it is mostly due to the acoustic phonons because the electron contribution to K is negligible [32]. It is estimated from the Wiedemann–Franz law which is an experimental discovery that the ratio of the thermal to the electrical conductivity in several materials is approximately the same at the same temperature [33]. CNTs can be regarded as long ballistic conductors while conducting current and heat ballistically [34]. In the PCM nanocomposites, phonons are transported from one particle to another via the paraffin matrix in between. Hence, the resistance to the heat flow caused by paraffin–CNT interface is a key factor for the thermal conductivities of these PCM composites because these inclusions are small in size and their surface-to-volume ratios are large.

To elucidate the role of chemical modification, thermal conductivities of modified and pristine MWCNT embedded nanocomposites are presented as a function of mass fraction in Table 3. The measurements for solid and liquid phases were performed at 26ºC and 51ºC, respectively. In general, the liquid-phase thermal conductivities are lower than the corresponding solid-phase data for both modified and pristine MWCNTs. This is attributed to the breakage of orderly solid structure and destruction of crystallinity during the solid phase transition to the disordered liquid structure [7]. Pure paraffin wax showed thermal conductivity of 0.15 W/mK in liquid phase and 0.2 W/mK in solid phase.

It can be seen that the introduction of MWCNTs improved the thermal conductivity of the neat paraffin. The phonon transport can be assumed to occur preferably through MWCNTs, due to the higher number of phonon vibrational modes and the higher free length of path in the crystalline graphite structures, compared to paraffin wax [30]. Although there no significant change in thermal conductivity after modifying the MWCNT, the addition of silanized MWCNTs seems to be slightly more efficient in both solid and liquid phases.

The thermal conductivity enhancement in solid phase is nearly consistent with that in liquid phase, both for modified and pristine MWCNT PCM samples. As there is a difference in acoustic properties of the paraffin and pristine MWCNTs, and they interact with each other only through Van der Waals forces, only low frequency phonon vibration modes are available to carry a small amount of heat energy. The high frequency phonons which are the major energy carriers interact with other phonons before they could be transferred to some low energy vibrations states to couple with the matrix [12].

Table 3. Thermal conductivity of PCM nanocomposites at different loadings of modified and pristine MWCNTs

	MWCNT Modification	0.1 wt.%	0.5 wt.%	1 wt.%
Solid Phase	Pristine MWCNT	0.221	0.232	0.256
	Modified Si-MWCNT	0.232	0.241	0.261
Liquid Phase	Pristine MWCNT	0.166	0.172	0.189
	Modified Si-MWCNT	0.172	0.179	0.193

The thermal conductivity enhancement ratios (*KR*) of the PW/Si-MWCNT and PW/MWCNT composites were calculated according to KR (%) = $[(K_{PCM}-K_0)/K_0] * 100$, in which K_{PCM} and K_0 represent the thermal conductivities of composites and neat PW, respectively. Fig. 6. shows KR values at different loadings of MWCNTs in solid and liquid state.

Figure 6. Thermal conductivity enhancement ratios KR of the PW/Si-MWCNT and PW/MWCNT composites in a) solid phase b) liquid phase

As expected, PCM composites filled with 1 wt.% of modified MWCNTs showed the largest thermal conductivity enhancement up to 30% in solid phase. The silane coupling treatment can bridge the connection of Si-MWCNTs to the PW matrix and decrease the resistance to the heat flow caused by the interface.

3.6. Rheological characterization

As it was mentioned before, adding nanoparticles to the paraffin makes the PCM nanocomposites unstable under consecutive solid-liquid phase change with significant precipitation of the nanoparticles. One of the main objectives of surface modification in this study was to make a stable MWCNTs dispersion within the PW matrix. Small amplitude oscillatory shear (SAOS) rheological experiment is a well-practiced method to study structural changes associated with the addition of nanoparticles into the nanocomposites [35]. In order to find the effect of modification on the PCM stability, SAOS experiments in the temperature sweep mode were performed. The corresponding material functions, i.e. storage and loss moduli and complex viscosity were measured as a function of temperature for the neat paraffin and PCM nanocomposites containing 0.5wt.% and 1wt.% of modified and pristine MWCNTs. In the first run of the experiment, temperature increased from 40ºC to 80ºC. In the second run, the reverse action performed from 80ºC to 40ºC, and in the last run the temperature was again changed in the range of 40 ºC to 80ºC. Fig.7 shows the changes of the complex viscosity for the PCM nanocomposites.

Figure 7. Complex viscosity in three runs of temperature sweep rheometry for a) neat paraffin wax, PCM nanocomposites with 0.5 wt.% b) pristine MWCNT c) silanized MWCNT, with 1wt.% d) pristine MWCNT e) silanized MWCNT

In Fig 7.a, the complex viscosity of the neat paraffin is plotted as function of temperature. As expected, there is no gap between the first, second and the last run of the experiment; as there is no filler in the neat paraffin to agglomerate. In Fig 7.b representing the data for the PCM containing 0.5 wt.% of pristine MWCNTs, a gap between complex viscosities in different runs can be observed. When the temperature raises heading to the liquid phase, the MWCNTs that interacted with paraffin only by Van der Waals forces agglomerate which results in a change in the viscosity of the PCM. This difference in the viscosity is a sign of instability. On the contrary, this gap cannot be seen in Fig 7.c indicating that the PCM incorporating 0.5wt.% of silanized MWCNTs is stable. Since the interfacial bonding between the Si-MWCNT and the paraffin is improved by the surface treatment, the Si-MWCNTs are stable and do not precipitate under the cyclic phase change. Similarly, Fig 7.d and 7.e, confirm the formation of stable PCMs for the samples with 1wt.% loadings of pristine and Si-MWCNT.

In the Fig. 8, the complex viscosities of the samples at 50°C in the first run are compared as a function of loading for modified and pristine samples. The modified MWCNTs exhibit lower viscosity as compared to the pristine MWCNTs over the whole range of filler loadings. The complex viscosity for samples containing 0.5 wt.% of pristine MWCNT is 20 times more than that of the PCMs loaded with 0.5 wt.% Si-MWCNT. As shown in the figure, the same observation can also be seen for 1 wt.% loading of nanotubes with a higher difference of 80-fold. Higher complex viscosity for samples containing pristine MWCNT may be due to the formation of a network type micro-structure, reducing the mobility of paraffin molecules when it is compared to the silanized MWCNT embedded nanocomposites [27].

Figure 8. Complex viscosity at 50°C in the first run of the experiment for the PCM nanocomposites

Obviously, the reason pertains to the silanization process. The anchored ODMS on the MWCNTs surface introduces an additional "soft layer", which prevents the agglomeration of MWCNTs and subsequently improves their dispersion quality. Reduction in the viscosity can be due to the slippage while the higher viscosity of PCM containing pristine MWCNTS can be assigned to MWCNTs agglomeration [35]. The better MWCNT dispersion promotes the alignment of the MWCNTs, which makes the PW easier to flow, and thus reduces the internal friction between hydrocarbon chains. A similar phenomenon is also reported by Zhu et al. for silane treated CNFs in epoxy resin nanocomposites [36], Tuteja et al. for fullerene and magnetite nanoparticles in polystyrene [37], Kaully et al. for $CaCO_3$ filled composites [38], and Mackay et al. for polystyrene nanoparticles in a linear polystyrene [39].

Acknowledgements

The authors would like to express their special thanks to Liane Häuβler for technical support.

Conclusions

In this work, a novel family of composite paraffin based PCMs filled with pristine and organo-silane modified MWCNTs was prepared and their thermal energy storage applications were comprehensively studied. FTIR analysis revealed that siloxane units have been added onto the surface of the MWCNTs during the silanization process. The melting/solidification enthalpies decreased moderately due to addition of pristine MWCNTs while the modified MWCNTs exhibited slightly favourable enhancement in these parameters. The melting/solidification temperatures remained nearly unchanged, with the maximum deviation being less than 0.5K. The results also showed that the electrical surface resistivity of the PCM composites decreased with the addition of pristine MWCNTs, achieving the minimum electrical resistivity value (882.7 Ω/square) at 1 wt.%. On the contrary, PCMs with embedded silanized MWCNTs were electrically nonconductive as the surface-attached functional groups greatly shifted the surface properties of Si-MWCNTs. The thermal conductivity of the nanocomposites increased with increasing the MWCNTs content by about 30% at the maximum loading of CNTs independent of the kind of CNTs. The temperature sweep rheological assessments also verified the higher stability of silanized MWCNTs dispersion as compared to that of the pristine MWCNTs within the novel composite PCMs showing the effectiveness of the MWCNT modification on the stability improvement which is highly important feature for development of composite PCMs. The organo-silane-modified MWCNT composite PCMs, with enhanced capability of thermal responses, may be considered as an inexpensive candidate for a variety of thermal energy storage applications.

References

1. Pielichowska, K.; Pielichowski, K. *Prog. Mater. Sci.* **2014**, *65*, 67.
2. Fang, X.; Fan, L.-W.; Ding, Q.; Yao, X.-L.; Wu, Y.-Y.; Hou, J.-F.; Wang, X.; Yu, Z.-T.; Cheng, G.-H.; Hu, Y.-C. *Energy Convers. Manag.* **2014**, *80*, 103.
3. Chu, S.; Majumdar, A. *Nature* **2012**, *488*, 294.
4. Rathod, M. K.; Banerjee, J. *Renew. Sustain. Energy Rev.* **2013**, *18*, 246.
5. Farid, M. M.; Khudhair, A. M.; Razack, S. A. K.; Al-Hallaj, S. *Energy Convers. Manag.* **2004**, *45*, 1597.
6. Cui, Y.; Liu, C.; Hu, S.; Yu, X. *Sol. Energy Mater. Sol. Cells* **2011**, *95*, 1208.
7. Shi, J. N.; Ger, M. Der; Liu, Y. M.; Fan, Y. C.; Wen, N. T.; Lin, C. K.; Pu, N. W. *Carbon N. Y.* **2013**, *51*, 365.
8. Warzoha, R. J.; Weigand, R. M.; Fleischer, A. S. *Appl. Energy* **2015**, *137*, 716.
9. Zalba, B.; Marín, J. M.; Cabeza, L. F.; Mehling, H. *Appl. Therm. Eng.* **2003**, *23*, 251.
10. Demirbas, M. F. *Energy Sources, Part B Econ. Planning, Policy* **2006**, *1*, 85.
11. Sharma, A.; Tyagi, V. V.; Chen, C. R.; Buddhi, D. *Renew. Sustain. Energy Rev.* **2009**, *13*, 318.
12. Wang, J.; Xie, H.; Xin, Z.; Li, Y.; Chen, L. *Sol. Energy* **2010**, *84*, 339.
13. Fan, L. W.; Fang, X.; Wang, X.; Zeng, Y.; Xiao, Y. Q.; Yu, Z. T.; Xu, X.; Hu, Y. C.; Cen, K. F. *Appl. Energy* **2013**, *110*, 163.
14. Xiang, J.; Drzal, L. T. *Sol. Energy Mater. Sol. Cells* **2011**, *95*, 1811.
15. Lee, J.-H.; Kathi, J.; Rhee, K. Y.; Lee, J. H. *Polym. Eng. Sci.* **2010**, *50*, 1433.
16. Berber, S.; Kwon, Y.-K.; Tomanek, D. *Phys. Rev. Lett.* **2000**, *84*, 4613.
17. Lee, G.-W.; Lee, J. I.; Lee, S.-S.; Park, M.; Kim, J. *J. Mater. Sci.* **2005**, *40*, 1259.
18. Tasis, D.; Tagmatarchis, N.; Bianco, A.; Prato, M. *Chem. Rev.* **2006**, *106*, 1105.
19. C. Velasco-Santos, A. L. M.-H. and V. M. C. *Silanization of Carbon Nanotubes : Surface Modification and Polymer Nanocomposites*; **2011**.
20. Wang, J.; Xie, H.; Xin, Z. *Thermochim. Acta* **2009**, *488*, 39.
21. Teng, T. P.; Cheng, C. M.; Cheng, C. P. *Appl. Therm. Eng.* **2013**, *50*, 637.
22. Hashempour, S.; Vakili, M. H. *J. Exp. Nanosci.* **2018**, *13*, 188.
23. Wang, J.; Xie, H.; Xin, Z. *J. Mater. Sci. Technol.* **2011**, *27*, 233.
24. Ma, P. C.; Kim, J.; Tang, B. Z. *Carbon N. Y.* **2006**, *44*, 3232.

25. Lehman, J. H.; Terrones, M.; Mansfield, E.; Hurst, K. E.; Meunier, V. *Carbon N. Y.* **2011**, *49*, 2581.

26. Wood, W.; Kumar, S.; Zhong, W. H. *Macromol. Mater. Eng.* **2010**, *295*, 1125.

27. Ehsan, R.; Babak, K. *J. Appl. Polym. Sci.* **2017**, *135*, 45740.

28. Cai, Y.; Hu, Y.; Song, L.; Tang, Y.; Yang, R.; Zhang, Y.; Chen, Z.; Fan, W. *J. Appl. Polym. Sci.* **2006**, *99*, 1320.

29. Lavorgna, M.; Romeo, V.; Martone, A.; Zarrelli, M.; Giordano, M.; Buonocore, G. G.; Qu, M. Z.; Fei, G. X.; Xia, H. S. *Eur. Polym. J.* **2013**, *49*, 428.

30. Gojny, F. H.; Wichmann, M. H. G.; Fiedler, B.; Kinloch, I. A.; Bauhofer, W.; Windle, A. H.; Schulte, K. *Polymer (Guildf).* **2006**, *47*, 2036.

31. Ma, P. C.; Kim, J.-K.; Tang, B. Z. *Compos. Sci. Technol.* **2007**, *67*, 2965.

32. Kim, P.; Shi, L.; Majumdar, A.; McEuen, P. L. *Phys. Rev. Lett.* **2001**, *87*, 19.

33. Lavasani, A.; Bulmash, D.; Das Sarma, S. *Phys. Rev. B* **2019**, *99*, 85104.

34. White, C. T.; Todorov, T. N. *Nature* **1998**, *393*, 240.

35. Aghjeh, M. R.; Asadi, V.; Mehdijabbar, P.; Khonakdar, H. A.; Jafari, S. H. *Compos. Part B Eng.* **2016**, *86*, 273.

36. Zhu, J.; Wei, S.; Yadav, A.; Guo, Z. *Polymer (Guildf).* **2010**, *51*, 2643.

37. Tuteja, A.; Duxbury, P. M.; Mackay, M. E. *Macromolecules* **2007**, *40*, 9427.

38. Kaully, T.; Siegmann, A.; Shacham, D. *Polym. Adv. Technol.* **2007**, *18*, 696.

39. Mackay, M. E.; Dao, T. T.; Tuteja, A.; Ho, D. L.; Van Horn, B.; Kim, H.-C.; Hawker, C. J. *Nat. Mater.* **2003**, *2*, 762.

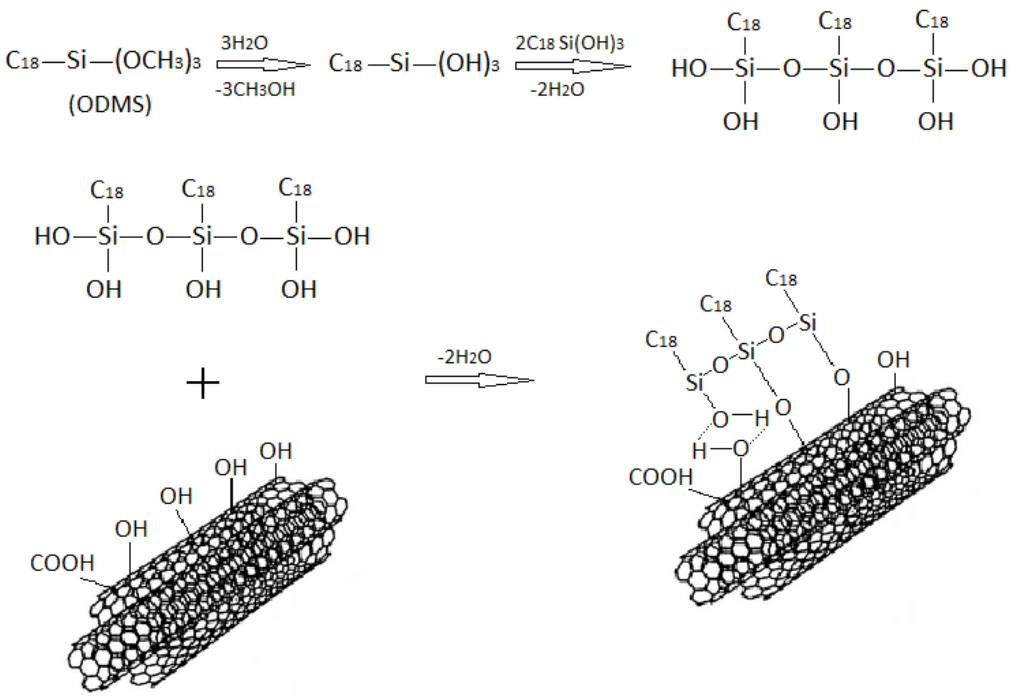

Figure 1. Schematic representation of silanization process of multi-walled carbon nanotubes

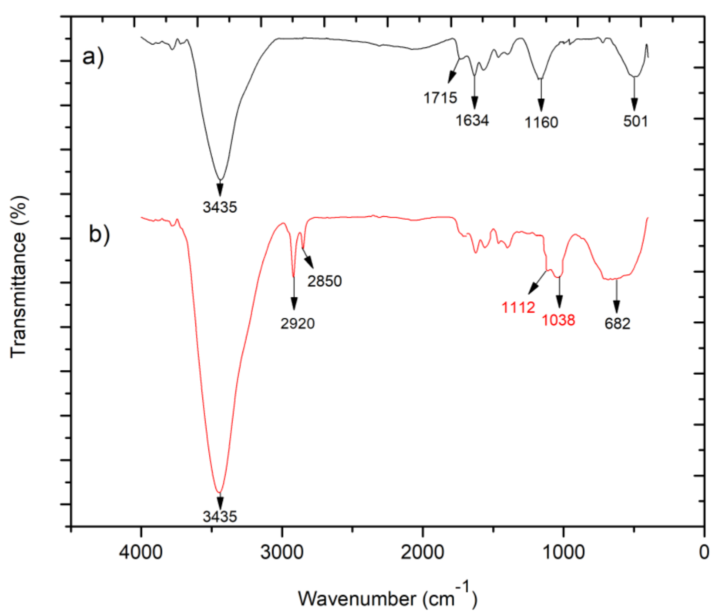

Figure 2. FTIR spectra of a) oxidized and b) silanized MWCNTs

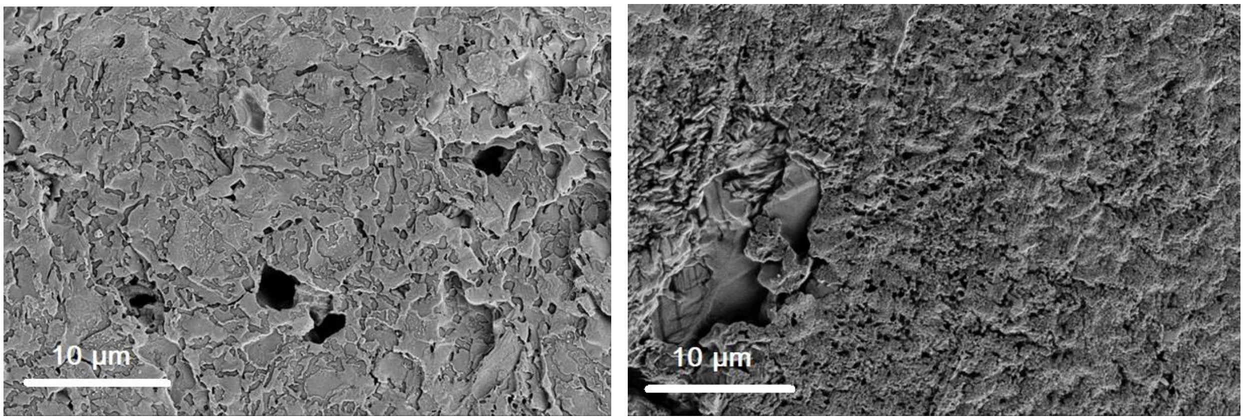

a) b)

Figure 3. SEM images of paraffin wax composites loaded with 0.5 wt.% of a) pristine MWCNT b) Si-MWCNT

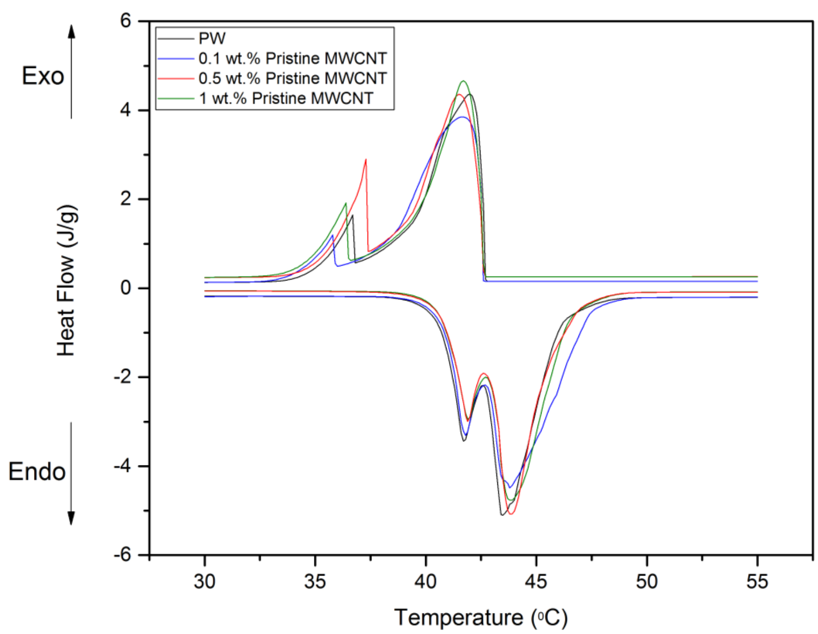

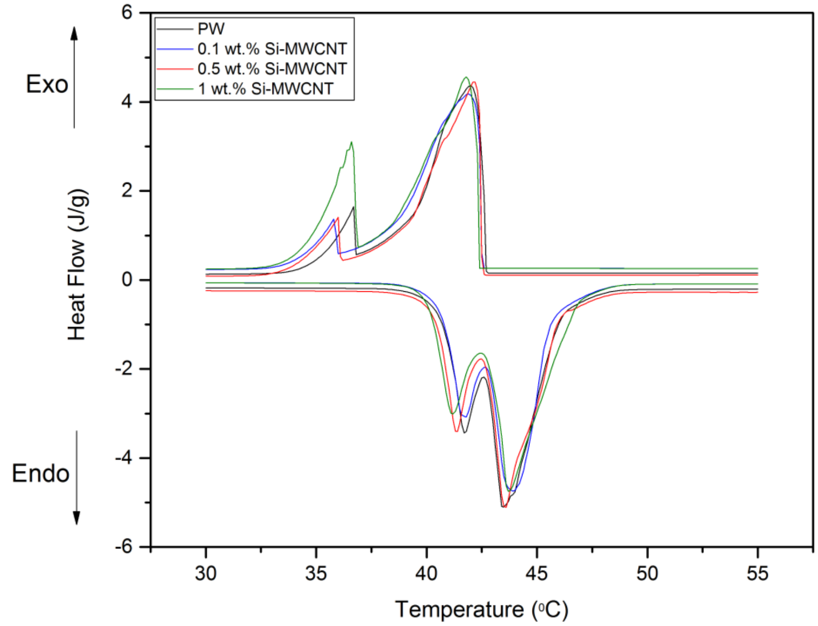

(b)

Figure 4. DSC curves (cooling and second heating) of the paraffin-based nanocomposite PCMs filled with a) pristine MWCNTs b) Si-MWCNTs

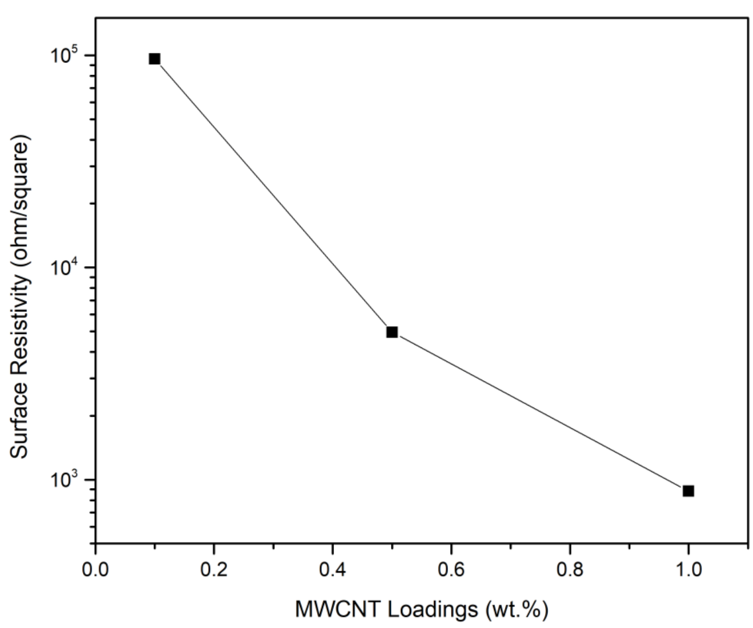

Figure 5. Electrical surface resistivity of pristine MWCNT/paraffin PCM nanocomposites

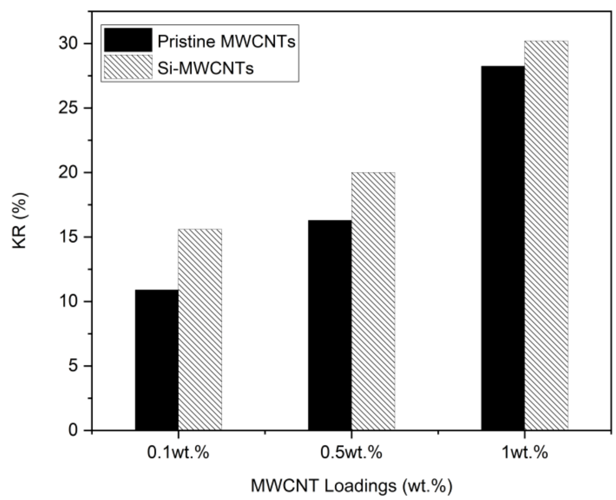

a)

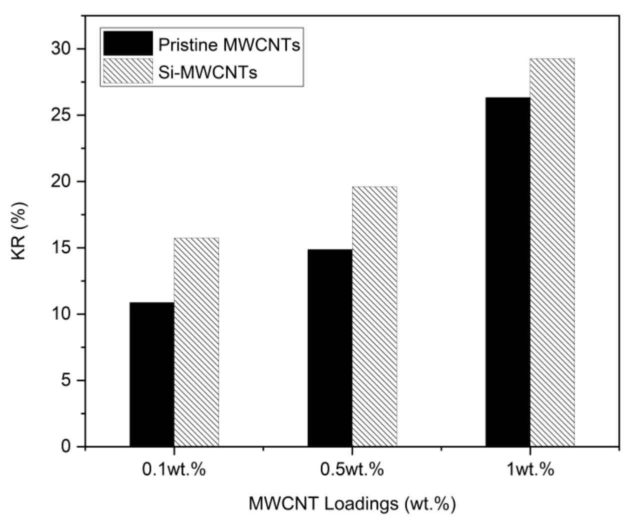

b)

Figure 6. Thermal conductivity enhancement ratios KR of the PW/Si-MWCNT and PW/MWCNT composites in a) solid phase b) liquid phase

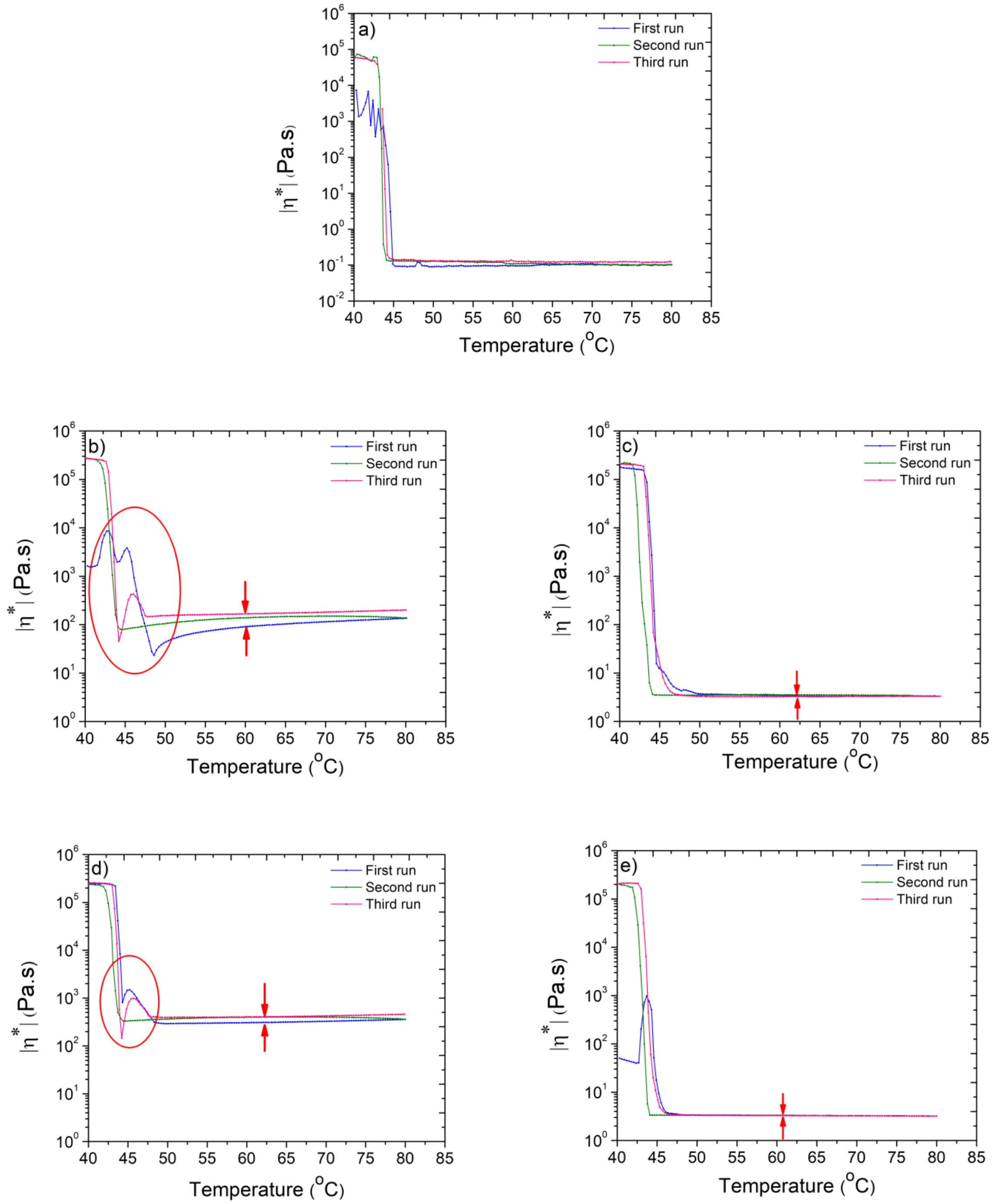

Figure 7. Complex viscosity in three runs of temperature sweep rheometry for a) neat paraffin wax, PCM nanocomposites with 0.5 wt.% b) pristine MWCNT c) silanized MWCNT, with 1wt.% d) pristine MWCNT e) silanized MWCNT

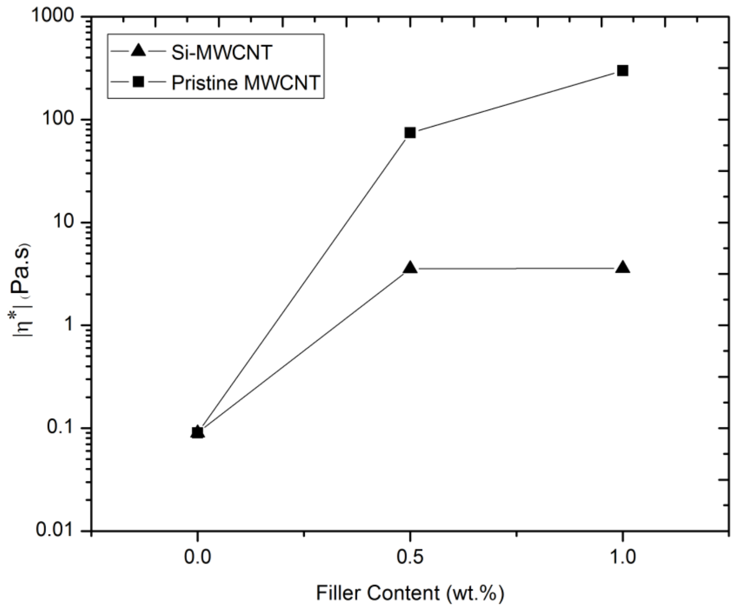

Figure 8. Complex viscosity at 50°C in the first run of the experiment for the PCM nanocomposites

Graphical Abstract Image